Communication

An Experimental Study of Stem Transported-Posture Adjustment Mechanism in Potato Harvesting

Jiali Fan [1], Yuyao Li [1], Weiwen Luo [1], Ke Yang [1], Zhaoyang Yu [1], Shenying Wang [2], Zhichao Hu [1,*], Bing Wang [3,4,*], Fengwei Gu [1] and Feng Wu [1]

1 Nanjing Institute of Agricultural Mechanization, Ministry of Agriculture and Rural Affairs, Nanjing 210014, China
2 College of Biosystems Engineering and Food Science, Zhejiang University, Hangzhou 311200, China
3 Graduate School of Chinese Academy of Agricultural Sciences, Beijing 100083, China
4 Key Laboratory of Modern Agricultural Equipment, Ministry of Agriculture and Rural Affairs, Nanjing 210014, China
* Correspondence: huzhichao@caas.cn (Z.H.); wangbing@caas.cn (B.W.)

Abstract: Potato stem removal is one of the critical technical problems of potato mechanized harvesting; it directly affects the quality of potato harvesting and potato storage. There have been several studies on potato stem removal mechanisms. In practice, however, it was found that the potato stem removal rate was greatly influenced by the posture of the stem before it entered the removal mechanism. In this study, we designed a potato stem posture adjustment mechanism consisting of elastic curtains. A test rig was built to investigate the effect of curtain height, curtain width, and curtain suspension height on potato passage rate and potato stem removal rate. The Box–Behnken design (BBD), combined with the response surface method, was used to conduct the test. The optimal construction and installation parameters for each elastic curtain were determined as 278.93 mm for the curtain height, 20 mm for the curtain width, and 260 mm for the curtain suspension height. The predicted values of potato passage rate and potato stem removal rate under the optimal parameters were 92.36% and 82.83%, which were consistent with the validation test results. Based on the optimization results, a rigid-flexible coupled simulation model for a potato stem transported-posture adjustment process based on Abaqus and Adams was constructed. The maximum impact of the elastic curtain of the stem posture adjustment mechanism on the potato stem was 15.91 N and caused the stem to spring back. The projection angle β' of the stem posture angle in the xoz plane before posture adjustment was $19.07°$, and the β' of the stem after posture adjustment was $87.18°$. At this time, the stem was basically parallel to the rod of the separating sieve and had a high probability of falling from the gap of the bar to complete the removal of the stem. Overall, the stem transport position adjustment mechanism effectively adjusted the stem transported posture and improved the stem removal rate in potato mechanical harvesting.

Keywords: potato harvester; potato stem transported-posture adjustment; potato stem removal; Box–Behnken Design; Abaqus–Adams Coupling Simulation

1. Introduction

Potato is the world's fourth largest food crop after maize, wheat and rice, with a global potato harvest area of 16,494,810 ha and production of 35,907,1403 tonnes in 2020 [1]. Moreover, potato is rich in dietary fiber, protein, trace elements, minerals, and vitamins and still has a high production potential, which is important to ensure world food and nutrition security [2,3]. Harvesting is the most labor-intensive part of potato production; therefore, potato mechanized harvesting technology has been a research hotspot for many scholars and enterprises. Potato–soil separation, potato stem removal, and potato block damage are the key obstacles for potato harvesters around the world in improving potato harvest quality.

To address the problem of potato–soil separation, much work has been done in terms of mechanism design, theoretical research, and simulation to obtain a high rate of separation [4–7]. However, compared to potato–soil separation, which mainly uses a rod separating sieve to screen the potato tubers from the soil, the mechanisms commonly used for potato stem removal are more complex and diverse. Potato stem residues have the potential to rot and transmit bacteria to the potato tubers during transport and storage, causing economic losses and food safety problems [8,9]. Therefore, improving the stem removal effect of existing potato harvesters is an urgent need to enhance the quality of potato mechanized harvesting and storage.

To solve the potato stem removal problem, several types of stem removers have been used in potato harvesting, such as the picking roller remover, spiral roller remover, and finger roller remover [10–12]. However, the posture of the potato stem when entering the remover has a great impact on the potato stem removal effect, which seriously limits the further improvement of the potato stem removal rate.

To solve this problem, we designed a new type of potato stem transported-posture adjustment mechanism using elastic curtains. We built a test rig to calculate the potato passing rate and stem removal rate for each combination of parameters, and optimized the parameters using the Box–Behnken design (BBD) and Response Surface Method. To further analyze the process, a rigid-flexible coupling simulation model was established.

2. Layout of Stem Remover and Influence of Stem Posture on the Stem Remover

2.1. Layout of Potato Stem Removal Mechanism in the Harvester

Among the various potato stem removers, the picking roller remover has great performance under high stem feeding conditions [13]. Figure 1 shows our self-developed hilly mountain potato combine harvester, which is equipped with a picking roller remover. The excavation depth of the excavation shovel is controlled by the depth limiting device at the front of the harvester. Potatoes are dug out from the soil by the excavation shovel. The separating rod sieve transports the potatoes backwards to remove impurities such as soil and stems, retaining the potato tubers. The potato stem removal mechanism consists of stem guide bars and a grooved stem picking roller, as shown in the red dashed box in Figure 1.
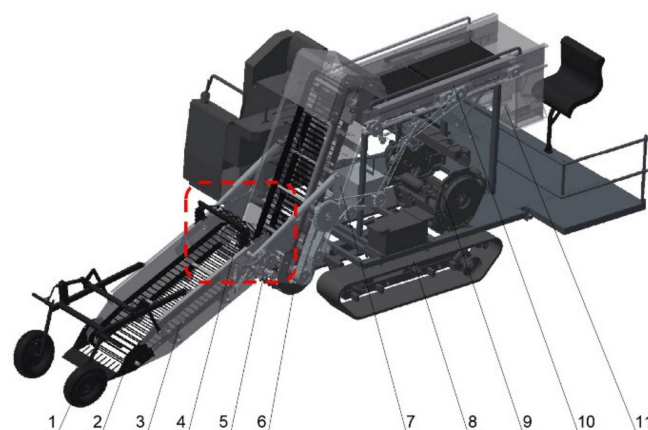

Figure 1. Structure diagram of the small self-propelled potato combine harvester. 1. Depth limiting device; 2. Excavation shovel; 3. Separating rod sieve; 4. Stem guide bar; 5. Grooved stem picking roller; 6. Curved handing part; 7. Lifting and conveying mechanism; 8. Tracked chassis; 9. Engine; 10. Selecting table; 11. Potato collection device.

The lifting and conveying mechanism elevates the potatoes to the selecting table for further selection. Potatoes are transported to the potato collection device for bagging after selection. Due to the restricted space structure, the whole machine has only one opportunity for stem removal. Poor stem removal seriously affects the harvesting quality. Therefore,

the potato stem remover is one of the critical devices of the potato combine harvester, and the improvement of its performance is the key to achieve mechanized potato production in small fields of hilly mountainous areas.

2.2. Effect of Potato Stem Transported Posture on the Picking Roller Stem Remover

We use the picking roller stem remover as an example to illustrate the effect of stem transported posture on potato stem removal performance, as shown in Figure 2. In ideal conditions, the stems are guided by the stem guide bar to the gap between the separating rod sieve and the grooved stem picking roller. The stem picking roller is rotated in the opposite direction to the separating rod sieve active shaft, pulling the potato stems out from the gap. The potatoes pass directly by the gap of the stem guide bar and continue to be transported backwards.
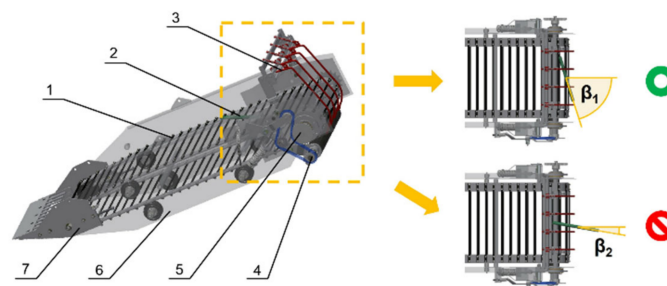

Figure 2. Schematic diagram of the structure and failure situation of the picking roller stem remover. 1. Separating rod sieve; 2. Potato stem; 3. Stem guide bar; 4. Grooved stem picking roller; 5. Separating rod sieve active shaft; 6. Rack; 7. Excavation shovel.

However, we found the potato stems were fed into the machine in different postures during the actual harvesting. Therefore, even equipped with a picking roller stem remover, there were still some stems that could not be removed because their posture angle was too small and let them directly pass through the gap between the stem guide bars. The left side of Figure 2 shows the structure of the picking roller stem remover. The top view of the stems passing through the stem removal mechanism is shown on the right side of Figure 2. When the stem posture angle β is larger, such as β_1, the stem can be successfully captured by the stem guide bars and smoothly enters the stem removal gap between the separating bar screen and the grooved stem picking roller for removal. When the stem posture angle β is small, such as β_2, the stem guide bars cannot stop the stem, and the stem is continuously transported backward through the gap of the stem guide bars, resulting in the failure of this stem removal mechanism. Hence, designing a mechanism that can effectively adjust the potato stem transported posture is key to improving the performance of the stem removal mechanism.

3. Materials and Methods

3.1. Design of Stem Transported-Posture Adjustment Mechanism in Potato Harvesting

The potato stem posture adjustment mechanism consisted of multi-stage hooks, a curtain hanging plate, and elastic curtains, as shown in Figure 3. Multi-stage hooks were fixed to the frame, with multiple hooks to accommodate different curtain hanging heights. The hanging height of the elastic curtain was less than the height of the curtain. When the stems transported by the separating rod sieve hit the rebounding elastic curtains at a small posture angle, they will rebound and increase the posture angle. In addition, stems with larger posture angles are mostly dropped from the rod gaps before being transported to the stem posture adjustment mechanism. Stems are susceptible to being adjusted by the mechanism for transport posture due to their lighter mass and lower kinetic energy. Potatoes are able to pass through the mechanism without much obstruction due to their larger mass and higher kinetic energy.
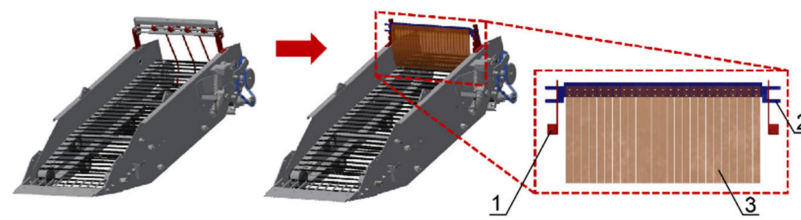
Figure 3. Schematic diagram of the stem transported-posture adjustment mechanism. 1. Multi-stage hook; 2. Curtain hanging plate; 3. Elastic curtain.

In order to achieve a better stem posture adjustment performance, minimize damage to potatoes, extend the working life of the mechanism and reduce the cost of production, the material of the elastic curtain should have the characteristics of good elasticity, wear resistance and low cost. Through experimental research, the material of the elastic curtain was chosen to be polyurethane, which has the characteristics of high elasticity and wear resistance [14–16].

3.2. Test Bench Construction and the Experimental Process

During field harvesting, the connection force between the potato and the stem was extremely weak, and most of the potatoes were disconnected from the stems by the vibrations generated during the excavation and the transportation. The potatoes were ellipsoidal in shape and became embedded in the gap between the rods, causing greater friction during the transportation process. The crushed soil leaked down through the gaps in the rods of the separation sieve to complete the separation. After mechanized haulm killing, the chopped stems were removed by dropping from the gap between the rods during the transportation process. However, long stubble stems with small posture angles were supported by several rods and continued to be transported backwards. The main objective of the potato stem transported-posture adjustment mechanism was to remove the long stubble stems with small posture angles while minimizing the obstruction to potato transport.

The potato stem transported-posture adjustment mechanism was tested for potato passing performance and stem removal effect, and the parameters of the mechanism were optimized. The potato and stem test samples were collected from Zhangye City, Gansu Province, China (38°33′36″ N,100°15′36″ E). Potato specimens were hand-dug from the fields, and selected undamaged individuals were sent back to the laboratory for testing. After mechanical haulm killing, the main stems of the stubble were manually pulled out from the field for testing.

The potato stem transported-posture adjustment mechanism test bench consisted of the potato harvester's power system, stem transported-posture adjustment mechanism, receiving bag, high-speed photography (HiSpec 5, FASTEC, San Diego, CA, USA), light source, and computer, as shown in Figure 4. The harvesting speed of this potato harvester was about 1 m/s. To fit the actual harvesting situation, a group of 5 potatoes was fed at a speed of 3 groups per second, with a total of 30 groups fed in each test. The potato passing rate was calculated from the number of potatoes in the receiving bag. The stems were fed at the stem posture angle of 10~20 degrees to ensure that the stems were not removed prematurely. They were fed at a feeding speed of 3 plants per second, with a total of 30 potato stems fed to each group. The potato stems in the receiving bag were those stems that failed to be removed and were used to calculate the stem removal rate for each group.

High-speed photography was used to capture the movement during the experiment, as shown in Figure 5. The potatoes were large in mass, high in momentum, and ellipsoidal in shape, with the lower part of the tubers embedded in the gaps of the rods during the conveying process. When passing through the potato stem transported-posture adjustment mechanism, the potato was able to resist the rebound of the elastic curtain and push the curtain to pass through. The stems were light and were supported by several rods with low frictional forces, which could not pass through the curtains. Then stems were rotated by the rebounding curtain and the stem posture angle increased until the stems were almost

parallel to the rods. Stems in this posture would most likely drop through the gaps of the rods and be removed from potatoes.
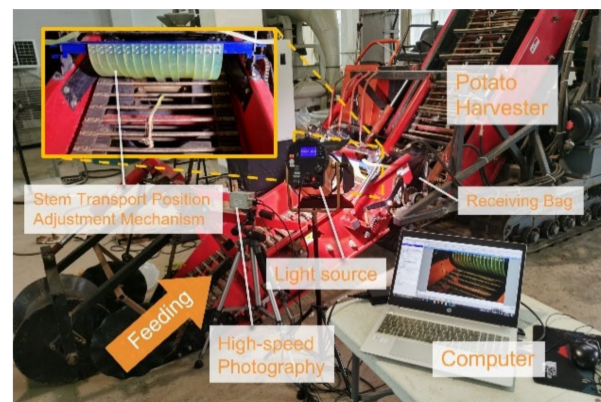

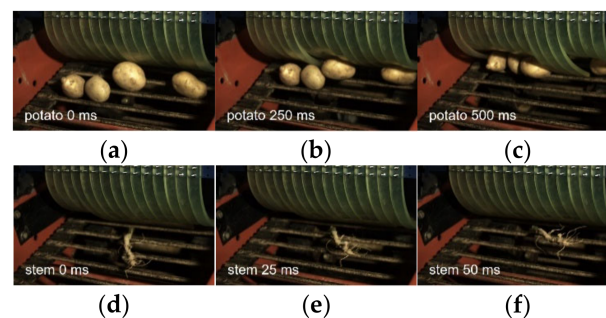**Figure 4.** The stem transported-posture adjustment mechanism test bench.

Figure 5. High-speed photographic images of potatoes and stems passing through the potato stem transported-posture adjustment mechanism. (**a–c**) Images of potatoes in contact with the stem posture adjustment mechanism for 0 ms, 250 ms and 500 ms. (**d–f**) Images of stems in contact with the stem posture adjustment mechanism for 0 ms, 25 ms and 50 ms.

3.3. Factors Selection and Experimental Protocol Design

The parameters affecting the stem posture angle β were categorized into three groups. The first group comprised the working parameters of the potato harvester, which were confirmed by our preliminary work [17]. The linear velocity V_r of the separating rod sieve was 1.37 m/s, and the angle $θ$ between the rod slope and the horizontal surface was 17.5°. The second category comprised the potato stem parameters, which were tested using samples collected at origin. The third category comprised the parameters related to the stem transported-posture adjustment mechanism. The modulus of elasticity E_c of the curtain was determined by the material. The initial velocity of the curtain V_{c0} was determined by the separation rod sieve line velocity V_r and the gap between the rods. The thickness of the curtain was determined to be 10 mm in pre-experiments. Therefore, only three factors remained to be determined and optimized through experiments, including the curtain height h, the curtain width a, and the curtain suspension height n.

The Box–Behnken design (BBD) is an experimental design method widely used in various fields for parameter optimization; it can replace full-scale tests with fewer test points [18–20]. In this study, a 3-factor, 3-level BBD test was selected, and the central group was set to 5 groups, with 17 groups of total experiments. The factors were the curtain height (X_1), the curtain width (X_2), and the curtain suspension height (X_3). The response values were potato passing rate (Y_1) and stem removal rate (Y_2). The levels of the factors and their codes are shown in Table 1.

Table 1. Levels and codes of experimental factors.

Level	Experimental Factors		
	Length of Curtain (X_1)	Width of Curtain (X_2)	Hanging Height of Curtain (X_3)
−1	270 mm	20 mm	240 mm
0	280 mm	25 mm	250 mm
1	290 mm	30 mm	260 mm

*3.4. Construction of Simulation Model for Stem Transported-Posture Adjustment*

In recent years, many scholars have used finite element or discrete element simulation software to establish a rigid-flexible coupling simulation model [21–25]. To further investigate the mechanical and kinematic response of the potato stem posture adjustment process, the finite element model of stem flexible body and curtain flexible body were established by Abaqus finite element analysis software. A rigid-flexible coupling model of the stem transported-posture adjustment mechanism in potato harvesting was established in combination with Admas multi-body dynamics analysis software.

The flexible body model of the stem and curtain was established in Abaqus software (MSC Software Corp., Newport Beach, CA, USA). The stem was simplified to a cylinder with a diameter of 13.87 mm and a length of 156.42 mm, and the data were obtained from the actual measurement of 30 plant samples. The curtain dimensional parameters were obtained from the optimal parameters obtained from the bench test. Material parameter settings are shown in Table 2 [26–28].

Table 2. Potato stem and curtain material parameters.

Material	Density (kg/m³)	Young's Modulus (Mpa)	Poisson's Ratio
Potato Stem	1.034	12.38	0.28
Curtain	1.2	15	0.49

The model for the stem and curtain were imported in Abaqus, and a frequency analysis step and a substructure analysis step were created, with the output form selected as Admas. Fully fixed constraints were applied to the reference points in the frequency analysis step, and all degrees of freedom were retained in the substructure analysis step. The results of meshing and modal operations for the stem and curtain are shown in the red box in Figure 6. The mnf. files were exported as flexible body files coupled to Admas.
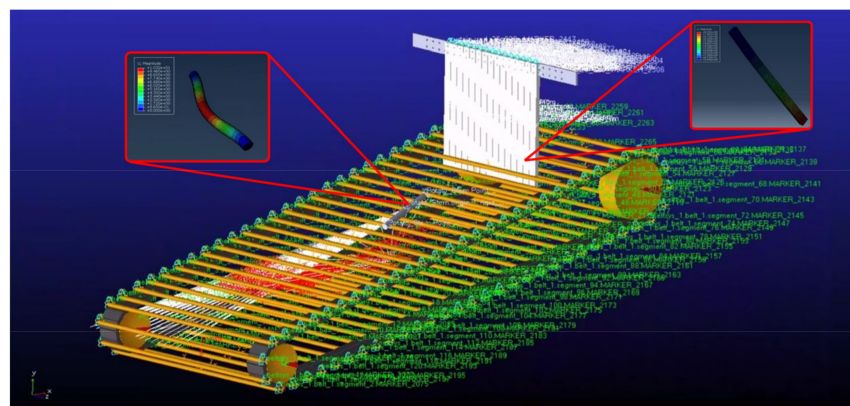
Figure 6. Rigid-flexible coupling simulation model of stem transported-posture adjustment process.

The separation rod sieve simulation model was built in Adams software (MSC Software Corp., USA). Each rod was a cylinder with a length of 560 mm and a radius of 10 mm.

The diameter of the driving wheel was 148 mm. The diameter of the driven wheel was 100 mm. The distance between the wheel center was 1055 mm, and the angle between the wheel center line and the horizontal plane was 17.5 degrees. Fixed rigid rods on the conveyor belt were set at 4 mm intervals. In order to make the linear speed of the separating rod sieve model consistent with the bench test, the main wheel speed was set to 1060.74°/s. The simplified model of the mechanism was imported, and the curtain was replaced with the mnf. flexible body file described as above. The stalk flexible body model and was imported, and the initial stem posture angle was set between 10 and 20 degrees. The total simulation time was 0.35 s, and the number of simulation steps was set to 3500. The rigid-flexible coupling simulation model of the potato stem transported-posture adjustment process is shown in Figure 6.

4. Results

4.1. Results of Stem Transported-Posture Adjustment Mechanism Bench Test

The results of the stem transport-position adjustment mechanism bench test are shown in Table 3. The multiple regression and the fitting analysis were performed by Design Expert software (Stat-Ease Inc., Minneapolis, MN, USA); the multiple regression equations are shown in Equations (1) and (2).

$$Y_1 = -3707.56 + 38.19X_1 + 36.69525X_2 - 14.49X_3 - 0.05X_1X_2 + 0.06X_1X_3 - 0.13X_2X_3 - 0.09X_1{}^2 + 0.20X_2{}^2 \quad (1)$$

$$Y_2 = 38.94 - 0.58X_1 - 0.50X_2 + 0.83X_3 \quad (2)$$

Table 3. Results of the stem transport-position adjustment mechanism bench test.

No.	Factors			Response Values	
	X_1	X_2	X_3	Y_1	Y_2
1	−1	−1	0	88.67	76.67
2	0	0	0	87.33	73.33
3	1	1	0	65.33	66.67
4	0	0	0	82.00	70.00
5	0	−1	−1	98.67	66.67
6	0	−1	1	95.33	83.33
7	0	0	0	90.67	73.33
8	−1	0	−1	95.33	70.00
9	−1	1	0	82.00	76.67
10	0	0	0	75.33	70.00
11	0	1	1	66.00	73.33
12	1	−1	0	82.67	70.00
13	1	0	1	66.00	73.33
14	−1	0	1	60.67	86.67
15	1	0	−1	76.00	53.33
16	0	0	0	84.67	70.00
17	0	1	−1	96.00	60.00

According to the software recommendations, the Quadratic model was chosen to fit the potato passing rate Y_1, and the Linear model was chosen to fit the stem removal rate Y_2. The difference in models was likely due to the fact that potatoes come into contact with multiple curtains during passing, while stems usually come into contact with only one single curtain. The ANOVA results for the experimental data are shown in Table 4. The model could be used for analysis and parameter optimization according to the results.

Table 4. ANOVA results for experimental data.

| Source | Y1 (Quadratic) | | | | Source | Y2 (Linear) | | | |
	Sum of Square	df	F Value	*p* Value		Sum of Square	df	F Value	*p* Value
Model	2141.5643	9	9.88	0.0032 **	Model	877.8223	3	48.07	<0.0001 **
X_1	168.0861	1	6.98	0.0333 *	X_1	272.3778	1	44.74	<0.0001 **
X_2	392.1400	1	16.28	0.0050 **	X_2	50.0000	1	8.21	0.0132 *
X_3	760.5000	1	31.58	0.0008 **	X_3	555.4445	1	91.24	<0.0001 **
X_1X_2	28.4622	1	1.18	0.3130					
X_1X_3	152.0289	1	6.31	0.0403 **					
X_2X_3	177.6889	1	7.38	0.0299 **					
$X_1{}^2$	373.3295	1	15.50	0.0056 **					
$X_2{}^2$	108.8190	1	4.52	0.0711 **					
$X_3{}^2$	0.0295	1	0.00	0.9730					
Residual	168.5895	7			Residual	79.1387	13		
Lack of fit	33.3939	3	0.33	0.8058	Lack of fit	65.8320	9	2.20	0.2328
Pure error	135.1956	4			Pure error	13.3067	4		
Cor Total	2310.1538	16			Cor Total	956.9609	16		
R^2 = 0.9270; Adjusted R^2 = 0.8332; Predicted R^2 = 0.6773					R^2 = 0.9173; Adjusted R^2 = 0.8982; Predicted R^2 = 0.8403				

Asterisks indicate significant difference at the (*) 95% and (**) 99% confidence levels.

From the results of the analysis, X_1, X_2, and X_3 in the primary term significantly affected the potato passing rate Y_1 and stem removal rate Y_2. In the interaction term, X_1X_3 and X_2X_3 significantly influenced the potato passing rate Y_1. In the secondary term, $X_1{}^2$, $X_3{}^2$ showed a significant effect on the potato passing rate Y_1. There were no interaction and quadratic terms for the stem removal rate, as it conformed to the Linear model. The effects of the interaction terms on the potato passing rate Y_1 are shown in Figure 7. The effects of single factor X_1, X_2, and X_3 on potato stem removal rate Y_2 are shown in Figure 8.

To improve the performance of the stem transported-posture adjustment mechanism for potato harvesting, the maximum potato passing rate Y_1 and the maximum potato stem removal rate Y_2 were used as the optimization objectives, with parameters ranging from −1 level to 1 level. The optimization equations are shown in Equations (3) and (4).

$$\begin{cases} \max Y_1(X_1, X_2, X_3) \\ \max Y_2(X_1, X_2, X_3) \end{cases} \tag{3}$$

$$\begin{cases} 270 \leq X_1 \leq 290 \\ 20 \leq X_2 \leq 30 \\ 240 \leq X_3 \leq 260 \end{cases} \tag{4}$$

The best combination of parameters was solved for 278.93 mm of curtain height, 20 mm of curtain width, and 260 mm of curtain suspension height, with the predicted potato passing rate of 92.36% and potato stem removal rate of 82.83%. The curtain height was rounded to 279 mm; both the curtain width and the curtain suspension height were taken as the optimal combination of parameters, and the test was repeated three times. The measured potato passing rates were 90.67%, 87.33%, and 91.33%, and the potato stem removal rates were 76%, 79.33%, and 86.67%. The test results were similar to the predicted values, indicating that the regression model established in this study was appropriate.

To simulate the performance of the potato stalk transport attitude adjustment mechanism in field harvesting with optimal parameters, potatoes and stems were randomly mixed and fed, and the potato passing rate and stem removal rate were determined. The experiment was repeated three times; the average potato passing rate was measured to be 92.22%, and the average stem removal rate was 88.67%. In contrast, there was no significant change in the potato passing rate, which may be attributed to the higher momentum of potatoes, which was less influenced by the stems.
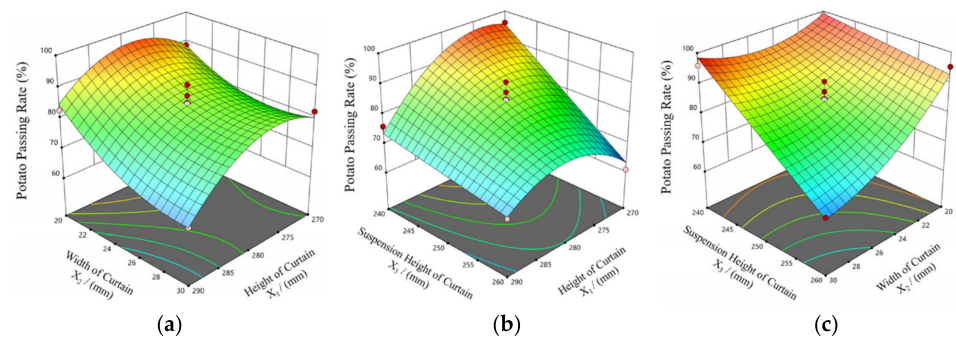
(a)   (b)   (c)

Figure 7. Response surface of interaction factors to coefficient of force on the potato Y_1. (**a**) Response surface under factors X_1 and X_2. (**b**) Response surface under factors X_1 and X_3. (**c**) Response surface under factors X_2 and X_3.
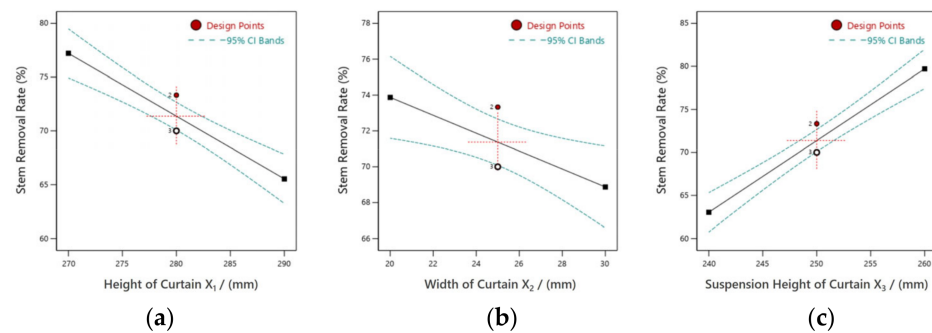

(a)   (b)   (c)

Figure 8. Curve of single factor effect on potato stalk removal rate. (**a**) Effect curve of the height of curtain (X1) on the stem removal rate. (**b**) Effect curve of the width of the curtain on the stem removal rate. (**c**) Effect curve of the hanging height of the curtain on the stem removal rate. The red dots represent the design points. The blue dotted lines represent the 95% confidence interval. The black curve is the effect curve of the single factor on the test value.

4.2. Analysis of Simulation Results for Potato Stem Posture Adjustment Process

We used simulation software to investigate the kinematics of the potato stem posture adjustment process; the process is shown in Figure 9. When the stem posture angle was small, the stem would be supported by several rods of the separating sieve to transport backwards, as shown in Figure 9a. The elastic curtain rebounded after impact by the rods. As the stem continued to be transported, the front of the stem contacted with the rebounding elastic curtain and was struck. The impact on the front of the stem caused the rotation of the stem, with the stem posture angle becoming gradually larger, as shown in Figure 9b,c. Under suitable parameters, the stem would collide with the rods while approximately parallel to the rods of the separating sieve and drop from the rod gap, as shown in Figure 9d. The simulation motion process was almost identical to the bench test.

Data exported from the Postprocessor module of ADAMS software are shown in Figure 10. Figure 10a shows the velocity and force diagram of the stem transported-posture adjustment process. The solid lines are velocity images. The solid red line in the figure is the image of the velocity of the center of mass of the stem in the *x*-axis direction. The solid blue line is the image of the velocity of the separation sieve bar in the *x*-axis direction. The dotted lines are force curves. The magenta dotted line is the force curve of the elastic curtain colliding with the stem. The brown, skyblue, and yellow dotted lines are the force curves of rod-stem collision. From the figure, it can be seen that the stem was transported by the rods of the separation sieve before contacting with the curtain, and the velocity of the center of mass was basically the same as that of the rods, with the velocity range of 1053.52 mm/s~1381 mm/s and an average value of velocity of 1223.75 mm/s. The peak force between the curtain and the stem during the contact with the elastic curtain was

15.91 N. After the end of the collision with the elastic curtain, three more collisions occurred with the rods of the separation sieve, with peak forces of 2.85 N, 12.82 N and 8.19 N.
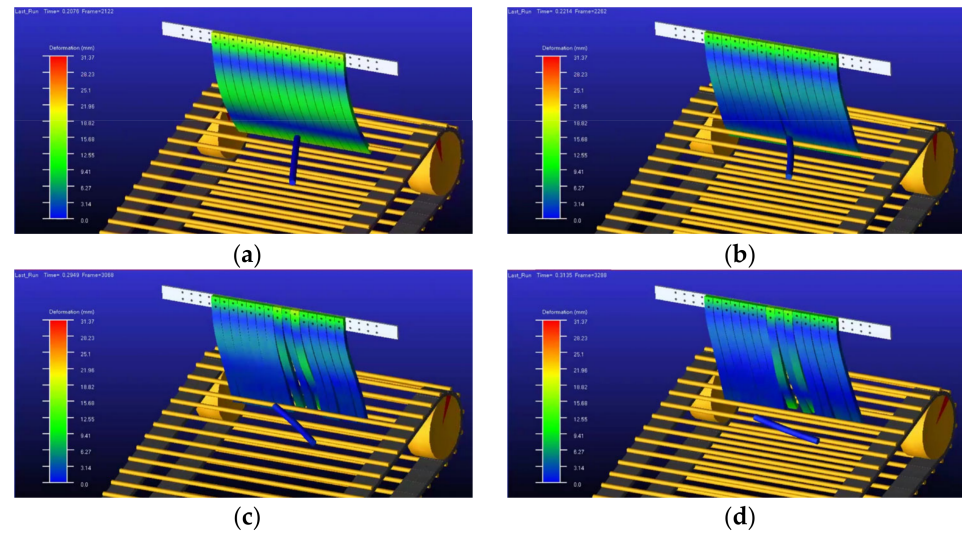

Figure 9. Simulation of potato stem transported-posture adjustment process. (**a**) Stem transported by separating sieve. (**b**) Stem colliding with elastic curtains. (**c**) Stem rebounding and separating from the elastic curtains. (**d**) Stem colliding with separating sieve rod.
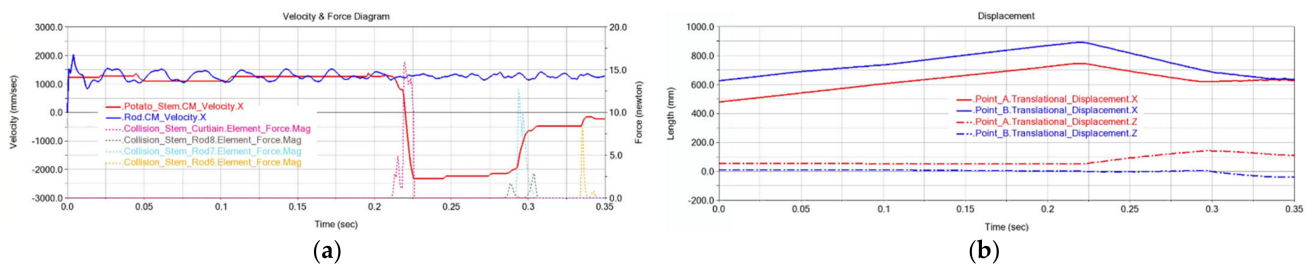

Figure 10. Simulation data exported from admas. (**a**) Velocity and force diagram of stem transported-posture adjustment process. (**b**) Displacement diagrams of the A and B marker points of the stem in the x−axis direction and z−axis direction.

The angle β' was assumed to be the projection angle of the stem posture angle β in the *xoz* plane. The schematic diagram of the projection angle β' for the stem posture angle is shown in Figure 11a. Marked points A and B were set at the center of the circle on both end faces of the stem, with point A far from the elastic stopper and point B close to the elastic curtain. The displacement curves of points A and B in the *x*-axis and *z*-axis derived from ADMAS are shown in Figure 10b.

The data of Figure 11b are used in Equation (5) to obtain the curve of the projection angle β' of the stem posture angle in the process of stem posture adjustment, as shown in Figure 11b.

$$\beta' = \arctan\left(\frac{A_z - B_z}{B_x - B_y}\right) \tag{5}$$

where β' is the projection angle of the stem posture angle β in the *xoz* plane. A_z is displacement of point A in the z-axis direction. B_z is displacement of point B in the z-axis direction. A_y is displacement of point A in the y-axis direction. B_y is displacement of point B in the y-axis direction.

As in Figure 11b, the initial projection angle β' of the stem was 16.57°. The stem projection angle β' had a slight increase during the transport of the separating rod sieve and was 19.07° before the collision with the elastic curtain. The stem projection angle β' sharply increased from 19.07° to 87.18° during the collision of stem with the elastic curtain

and the rebound of the stem. Finally, the stem collided with the rods of the separating sieve several times, and the angle fluctuated in the range of 86.98° to 87.22°; the probability of removing the stem by dropping from the gap between the rods was high in this posture.
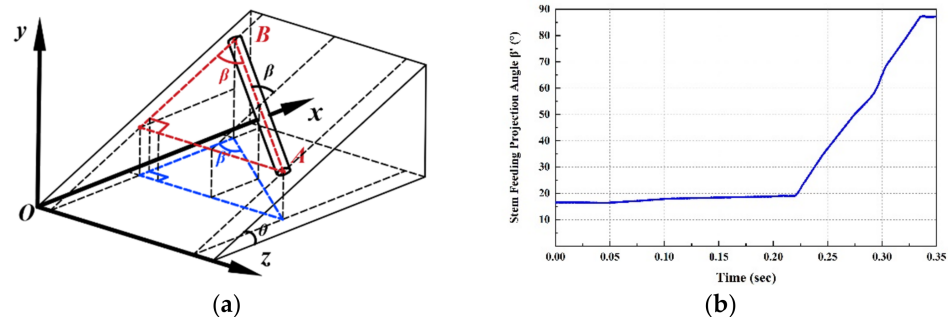

Figure 11. The schematic diagram and curve of the angle β'. (**a**) Schematic diagram of the stem posture angle β and its projection angle β'. (**b**) Curve of the projection angle β' during stem transported-posture adjustment process.

5. Conclusions

In this paper, an elastic curtain-type potato stem transported-posture adjustment mechanism was designed for the difficult problem of removing stems with a small posture angle in mechanized potato harvesting. The Box–Behnken design (BBD) experimental design method was used for parameter optimization of the bench test. The optimal parameters were determined as 278.93 mm for the curtain height, 20 mm for the curtain width, and 260 mm for the curtain suspension height. The predicted value of the potato passage rate was 92.36%, and the potato stem removal rate was 82.83% under the optimal parameters. The mechanism was effective in removing potato stems with small posture angle and high potato passing rate and could be applied to mechanical harvesting of potatoes after haulm killing.

A rigid-flexible coupled simulation model of Abaqus and ADMAS was built. According to the simulation results, the peak force of the stem in contact with the elastic stopper curtain was 15.91 N. During the stem rebound, the projection angle of the stem posture angle in the *xoz* plane increased sharply from 19.07° to 87.18°. The stems then collided three times with the rods of the separation sieve, and the projection angle fluctuated in the range of 86.98° to 87.22°. In this state, the stem was almost parallel to the rods of the separating screen, which made it easy to drop through the rod gaps of the separating sieve to complete the stem removal process. The simulation model provides a reliable and convenient method for the research of potato stem transported-posture adjustment mechanisms.

Author Contributions: Conceptualization, J.F., Y.L. and Z.H.; methodology, J.F., Y.L., Z.H. and Z.Y.; software, J.F. and S.W.; validation, Z.H., K.Y., F.G. and F.W.; formal analysis, J.F., Y.L. and W.L.; investigation, J.F., Y.L. and Z.Y.; resources, Z.H.; data curation, J.F. and Y.L.; writing—original draft preparation, J.F., Z.H. and F.G.; writing—review and editing, J.F., Z.H. and F.W.; visualization, J.F., W.L. and K.Y.; supervision, Z.H. and B.W.; project administration, Z.H. and B.W.; funding acquisition, B.W. All authors have read and agreed to the published version of the manuscript.

Institutional Review Board Statement: Not applicable.

Informed Consent Statement: Not applicable.

Data Availability Statement: The data presented in this study are available in the article.

Conflicts of Interest: The authors declare no conflict of interest.

References

1. FAOSTAT. Available online: http://faostat.fao.org (accessed on 4 June 2020).
2. Devaux, A.; Kromann, P.; Ortiz, O. Potatoes for sustainable global food security. *Potato Res.* **2014**, *57*, 11. [CrossRef]
3. Haverkort, A.J.; Struik, P.C. Yield levels of potato crops: Recent achievements and future prospects. *Field Crops Res.* **2015**, *182*, 76–85. [CrossRef]
4. Bulgakov, V.; Ruzhylo, Z.; Fedosiy, I.; Ivanovs, S. Experimental research and justification of parameters of spiral potato cleaner from admixtures. In Proceedings of the International Scientific Conference Engineering for Rural Development, Jelgava, Latvia, 20–22 May 2020.
5. Jinqing, L.; Xiaohan, Y.; Yining, L.; Zihui, L.; Jicheng, L.; Changlin, D. Analysis and Experiment of Potato Damage in Process of Lifting and Separating Potato Excavator. *Nongye Jixie Xuebao/Trans. Chin. Soc. Agric. Mach.* **2020**, *51*, 103–113. [CrossRef]
6. Wei, Z.; Li, H.; Sun, C.; Su, G.; Liu, W.; Li, X. Experiments and Analysis of a Conveying Device for Soil Separation and Clod-Crushing for a Potato Harvester. *Appl. Eng. Agric.* **2019**, *35*, 987–996. [CrossRef]
7. Wei, Z.; Niu, Q.; Li, H.; He, J.; Liu, W.; Hu, H.; Zhao, H. Design and analysis of wave shaped separation device of potato-soil for potato harvester. In Proceedings of the 2018 ASABE Annual International Meeting, Detroit, MI, USA, 29 July–1 August 2018; p. 1.
8. Daami-Remadi, M.; Jabnoun-Khiareddine, H.; Sdiri, A.; El Mahjoub, M. Comparative reaction of potato cultivars to Sclerotium rolfsii assessed by stem rot and tuber decay severity. *Pest Technol.* **2012**, *6*, 54–59.
9. De Boer, S.; Li, X.; Ward, L. Pectobacterium spp. associated with bacterial stem rot syndrome of potato in Canada. *Phytopathology* **2012**, *102*, 937–947. [CrossRef]
10. Liu, P.; Liu, Z.; Pei, C.; Yang, L.; Zhang, S.; Duan, M. Design optimization and Reliability Analysis of Hydraulic Cleaning System for Potato Harvester. In Proceedings of the 2019 International Conference on Quality, Reliability, Risk, Maintenance, and Safety Engineering (QR2MSE), Zhangjiajie, China, 6–9 August 2019; pp. 1010–1018.
11. Nyborg, B.D.; Geyer, W.C. Cleaning and Separator System for Tubers. U.S. Patent 2010096301A1, 22 April 2010, 19 October 2009.
12. Wei, H.; Wang, D.; Lian, W.; Yang, X.; Huang, X. Development of 4UFD-1400 type potato combine harvester. *Trans. Chin. Soc. Agric. Eng.* **2013**, *29*, 11–17.
13. Jinqing, L.; Pengrong, W.; Zhifeng, L.; Zihui, L.; Fayi, Z.; Deqiu, Y. Design and Experiment of Potato Harvester Potato Stem Separation Equipment. *Nongye Jixie Xuebao/Trans. Chin. Soc. Agric. Mach.* **2019**, *50*. [CrossRef]
14. Ashrafizadeh, H.; Mertiny, P.; McDonald, A. Evaluation of the effect of temperature on mechanical properties and wear resistance of polyurethane elastomers. *Wear* **2016**, *368–369*, 26–38. [CrossRef]
15. Das, A.; Mahanwar, P. A brief discussion on advances in polyurethane applications. *Adv. Ind. Eng. Polym. Res.* **2020**, *3*, 93–101. [CrossRef]
16. Sato, S.; Yamaguchi, T.; Shibata, K.; Nishi, T.; Moriyasu, K.; Harano, K.; Hokkirigawa, K. Dry sliding friction and Wear behavior of thermoplastic polyurethane against abrasive paper. *Biotribology* **2020**, *23*, 100130. [CrossRef]
17. Li, Y.; Hu, Z.; Gu, F.; Wang, B.; Fan, J.; Yang, H.; Wu, F. DEM-MBD Coupling Simulation and Analysis of the Working Process of Soil and Tuber Separation of a Potato Combine Harvester. *Agronomy* **2022**, *12*, 1734. [CrossRef]
18. Ferreira, S.L.C.; Bruns, R.E.; Ferreira, H.S.; Matos, G.D.; David, J.M.; Brandão, G.C.; da Silva, E.G.P.; Portugal, L.A.; dos Reis, P.S.; Souza, A.S.; et al. Box-Behnken design: An alternative for the optimization of analytical methods. *Anal. Chim. Acta* **2007**, *597*, 179–186. [CrossRef] [PubMed]
19. Montgomery, D.C. *Desing and Analysis of Experiments*; John Wiley & Sons Ltd.: New York, NY, USA, 2001; p. 427.
20. Tang, H.; Xu, C.; Xu, W.; Xu, Y.; Xiang, Y.; Wang, J. Method of straw ditch-buried returning, development of supporting machine and analysis of influencing factors. *Front. Plant Sci.* **2022**, *13*, 967838. [CrossRef] [PubMed]
21. Bu, L.; Hu, G.; Chen, C.; Sugirbay, A.; Chen, J. Experimental and simulation analysis of optimum picking patterns for robotic apple harvesting. *Sci. Hortic.* **2020**, *261*, 108937. [CrossRef]
22. Tang, H.; Xu, C.; Qi, X.; Wang, Z.; Wang, J.; Zhou, W.; Wang, Q.; Wang, J. Study on Periodic Pulsation Characteristics of Corn Grain in a Grain Cylinder during the Unloading Stage. *Foods* **2021**, *10*, 2314. [CrossRef]
23. Tian, Z.; Ma, W.; Yang, Q.; Yao, S.; Guo, X.; Duan, F. Design and Experiment of Gripper for Greenhouse Plug Seedling Transplanting Based on EDM. *Agronomy* **2022**, *12*, 1487. [CrossRef]
24. Wang, T.; Liu, Z.; Yan, X.; Mi, G.; Liu, S.; Chen, K.; Zhang, S.; Wang, X.; Zhang, S.; Wu, X. Finite Element Model Construction and Cutting Parameter Calibration of Wild Chrysanthemum Stem. *Agriculture* **2022**, *12*, 894. [CrossRef]
25. Xie, L.; Wang, J.; Cheng, S.; Zeng, B.; Yang, Z. Optimisation and dynamic simulation of a conveying and top breaking system for whole-stalk sugarcane harvesters. *Biosyst. Eng.* **2020**, *197*, 156–169. [CrossRef]
26. Elleuch, R.; Elleuch, K.; Salah, B.; Zahouani, H. Tribological behavior of thermoplastic polyurethane elastomers. *Mater. Des.* **2007**, *28*, 824–830. [CrossRef]
27. Fan, J.; Li, Y.; Wang, B.; Gu, F.; Wu, F.; Yang, H.; Yu, Z.; Hu, Z. An Experimental Study of Axial Poisson's Ratio and Axial Young's Modulus Determination of Potato Stems Using Image Processing. *Agriculture* **2022**, *12*, 1026.
28. Pritz, T. The Poisson's loss factor of solid viscoelastic materials. *J. Sound Vib.* **2007**, *306*, 790–802. [CrossRef]